

**Politecnico di Milano**

**LABORATORIO DI PRESTAZIONI DEI VELIVOLI**  
AA 2024-2025

**Docenti:**  
**Croce Cacciola Calzoni**

## **Elaborato d'esame [D2]**

**Velivolo:**  
**Bombardier**  
**BD700 Global Express**

**Autori:**

<b>Matricola</b>	<b>Cognome</b>	<b>Nome</b>	<b>Firma</b>
<b>982585</b>	<b>Weerasinghe</b>	<b>Jeevana Tharinda</b>	<i>Jeevana Weerasinghe</i>

**Data di consegna: 24/08/25**

## Table of contents

1.	Aircraft characteristics .....	3
2.	Comparison with aircrafts in the same class .....	7
3.	Polar data.....	8
4.	Level flight performances .....	10
5.	Climb performances .....	12
6.	Flight envelope with climb performances.....	15
7.	Turning performances .....	17
8.	Flight envelope in coordinated turn .....	20
9.	Additional results .....	21

Parameter	Value	Unit
Aircraft weight	35000	kg
Wing surface area	94,9	m <sup>2</sup>

## 1. Aircraft characteristics

### 1.1

The Bombardier BD700 Global Express is a long-range twin-engine business jet manufactured by Bombardier Aviation. First announced in October 1991, its maiden flight was in October 1996, while it received its Canadian type certification in July 1998 and entered service in July 1999.

The Global Express was developed from the Canadair Challenger 600 and the Bombardier CRJ (sharing their fuselage cross section) with the aim to carry eight passengers and four crew for over 12'000 km at Mach 0.85. The development, a joint effort by Bombardier, Mitsubishi Heavy Industries and Rolls-Royce, made wide use of CAD software and computational fluid dynamics software.

To ensure the reliability of the aircraft, it was designed to use the minimum number of components possible, while still guaranteeing that no single failure would result in a diversion of a flight. Its safety was further enhanced by a dedicated maintenance computer that detects and isolates faults. As fly-by-wire required an expensive implementation and was met by concern by customers, as its use in commercial aircrafts was still relatively recent, a conventional mechanical flight control system was used in the first iteration of the aircraft.

Lightweight aluminium alloys and composite materials were chosen for the airframe, and while the fuselage cross section is the same as the Challenger 600 and the CRJ, new wings, tail and engine were developed to reach the speeds and the range required. In particular, the wing is a supercritical airfoil with a 35° sweep angle which features winglets, while the engines are two Rolls-Royce BR710A2-20 turbofans.

The cabin can accommodate 12 to 16 passengers, depending on the variant, while its flexible interior layout offers multiple customization options for operators. Further enhancements allow the Global Express to have an increased width at shoulder level and larger windows than its precursors. As a business jet, it aims to provide versatility, range, speed and field performance, while maintaining passenger comfort at the forefront. For its range, speed and high load capacity, it's a preferred choice for rapid intercontinental travel for wealthy individuals, corporations and governments.

Numerous variants have been produced:

- Global 5000: entering service in 2005, it's a shorter aircraft with reduced range and MTOW.
- Global Express XRS: entering service in 2006, it replaced the original Global Express, providing greater range at higher speeds, more fuel capacity, better cabin pressurization, improved take-off performance and the Enhanced Vision System (EVS) offering real time infrared images.
- Global 6000: entering service in 2012, it's a rebranded and upgraded Global Express XRS, with enhanced wing flexibility and an updated avionics system.
- Global 5500/6500: entering service between 2019 and 2020, the Global 5500 and 6500 are updates of the Global 5000 and 6000. They feature a revised wing, optimized for higher Mach, overhauled cabin and the engines were upgraded to the Rolls-Royce Pearl 15, which provides enhanced thrust and improved efficiency (up to 13% less fuel burned). They also feature a Combined Vision System (CVS), which merges the EVS with a Synthetic Vision System (SVS), providing digital imagery of the surrounding environment unaffected by weather or visibility conditions.
- Military Variants: many air forces have employed modified versions of the Global Express, mainly deployed as surveillance aircraft.

## 1.2

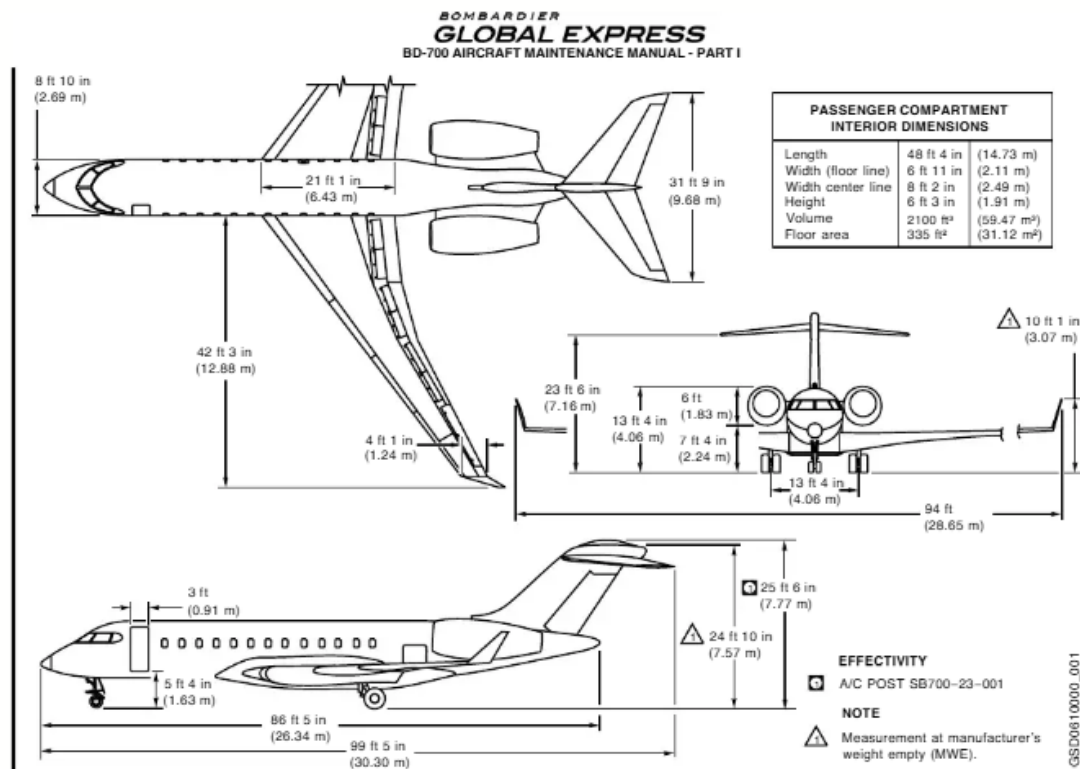
<b>Geometry</b>		
<b>Parameter</b>	<b>Value</b>	<b>Unit</b>
Length	30.3	m
Height	7.8	m
Wingspan	28.7	m
Wing chord (MAC)	4,42	m
Aspect ratio	8.68	-
Wing surface	94,9	$\text{m}^2$

<b>Weights</b>		
<b>Parameter</b>	<b>Value</b>	<b>Unit</b>
MTOW	45132	kg
ZWF	26308	kg
Typical TOW	35000	kg

<b>Powerplant: Rolls Royce Pearl 15</b>		
<b>Parameter</b>	<b>Value</b>	<b>Unit</b>
Engine type	Two shaft, high bypass turbofan	-
Static thrust	67.3	kN
Bypass ratio	4,8:1	-

<b>Basic performances</b>		
<b>Parameter</b>	<b>Value</b>	<b>Unit</b>
Max airspeed	Mach 0.9	-
Typical cruising speed	Mach 0.85	-
Operative ceiling	15545	m
Range	12223	km

## 1.3



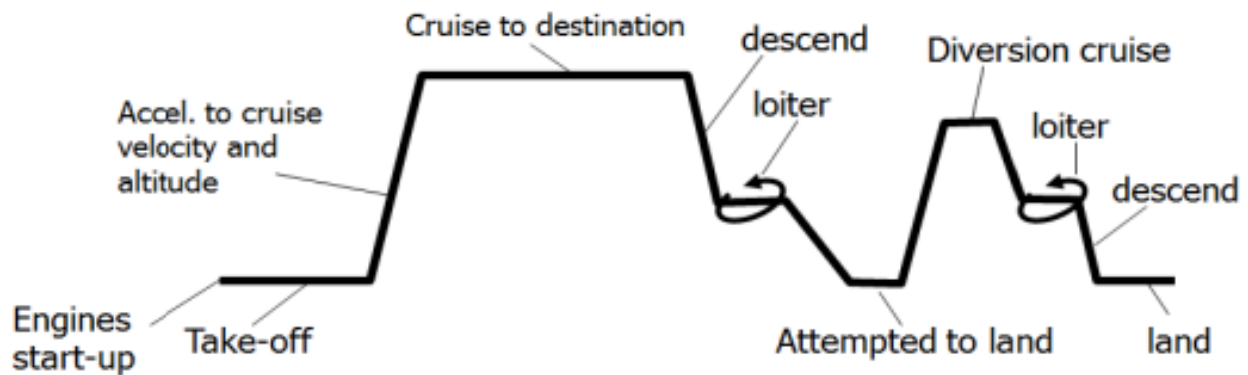
General Dimensions  
Figure 1

EFFECTIVITY: ALL

06-10-00

Page 5  
Nov 13/2017

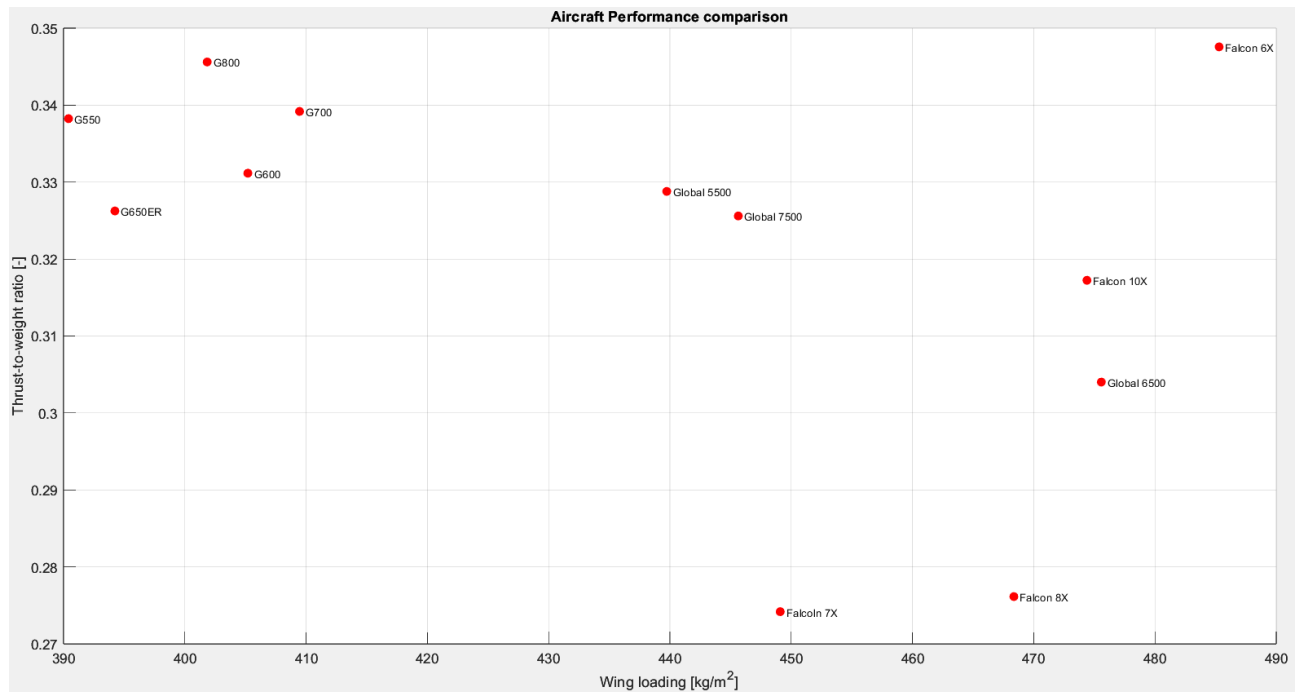
## 1.4



1. Take-off: having taxied to the runway and received take-off clearance, the aircraft accelerates to the rotation speed and lifts off initiating the climb. This phase is concluded when reaching a height above the runway surface of 35 ft (for CS25 planes).
2. Climb: the aircraft continues its ascent and accelerates until it reaches the planned initial cruising altitude, depending on weight and flight length.
3. Cruise: the aircraft travels at cruising speed and altitude. For longer flights, step climbs are used to climb to a higher altitude, which become more efficient as fuel is burned, and the aircraft becomes lighter.
4. Descend: the aircraft descends and decreases its speed following Standard Terminal Arrival Routes.
5. Loiter: the aircraft holds its altitude and circulates in a fixed pattern, usually under air traffic control instruction caused by airport congestion or weather conditions.
6. Landing attempt: the aircraft attempts a landing, which might not be completed. Unstable approach, obstructed runway, unfavourable weather conditions or a sub-optimal landing may require a go-around or a diversion.
7. Diversion: after a missed approach, it is possible to divert to an alternate airport. This involves a new climb, cruise and descent.
8. Landing: the aircraft successfully lands at the destination or alternate airport, followed by taxiing to parking.

## 2. Comparison with aircrafts in the same class

### 2.1



The Bombardier Global 6500 is characterized by a high wing loading and a relatively low thrust-to-weight ratio compared to other aircrafts in the same category. Being an aircraft highly optimized for long distance cruise at transonic speeds it presents a relatively smaller wing surface, decreasing drag at higher speeds. The thrust-to-weight ratio figure also indicates an optimization for cruising, with smaller and more efficient engines providing better fuel consumption. The apparently low take-off and landing performance is compensated by a large, flapped area.

The Global 5500 has the same wings and engines as the 6500 but has a shorter fuselage and a reduced range while the Global 7500, the largest business jet in production, has more powerful engines, a larger fuselage and increased range.

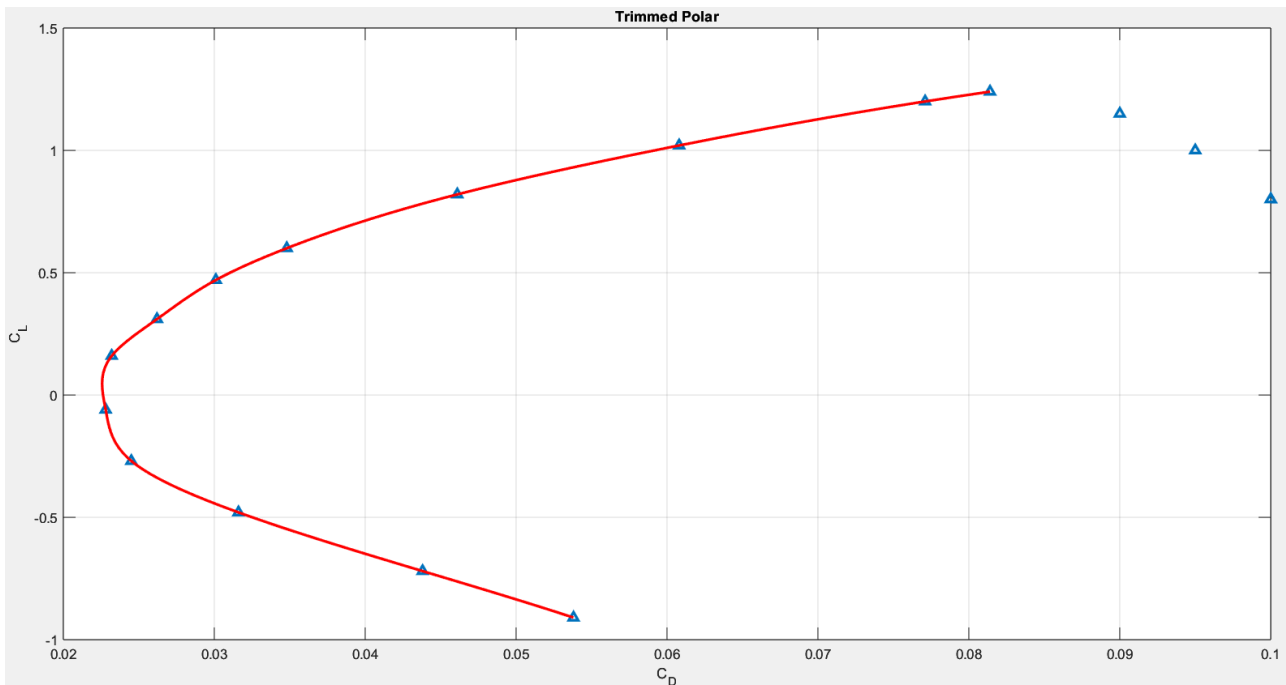
Of opposite design philosophy, the Gulfstream family focuses on providing superior take-off and landing performances, with large wing areas and relatively powerful engines that allow operations even from shorter runways.

The Dassault Falcon 7X and 8X are notable outliers: being trijets they employ engines of modest thrust compared to the other aircrafts but offer a significant level of safety in case of engine failure.

### 3. Polar data

From the given set of data, the points beyond the stall condition have been excluded.

#### 3.1

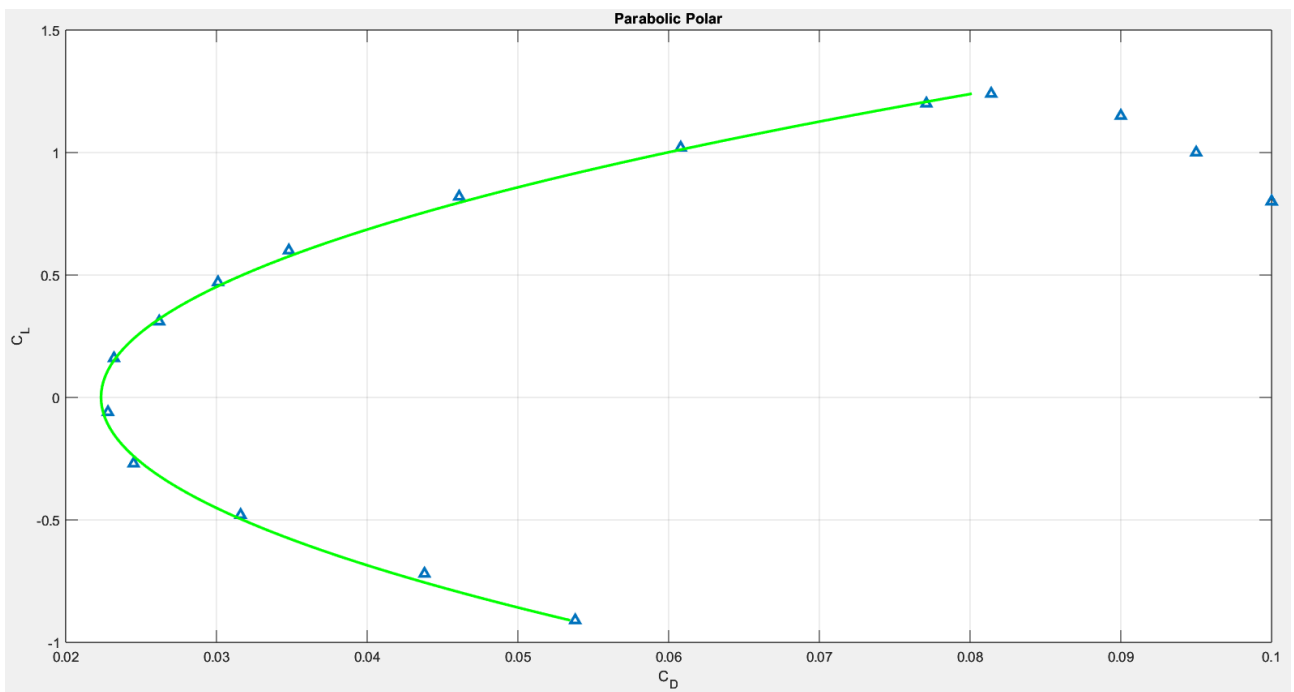


Spline interpolation of the polar data:  $y = \text{spline}(XX, YY)$ .

#### 3.2

Parameter	Value
$\max(C_L)$	1,2400
$\max(C_L/C_D)$	17,8705
$\max(C_L^{3/2}/C_D)$	17,0923
$\max(C_L^{1/2}/C_D)$	22,7895

### 3.3



Best fit with analytic model of parabolic polar  $C_D = C_{D0} + KC_L^2$  obtained with the MATLAB function  $y = polyval(polyfit(XX^2, YY, 1))$ .

### 3.4

Parameter	Value
$C_{D0}$	0.0223
K	0.0376

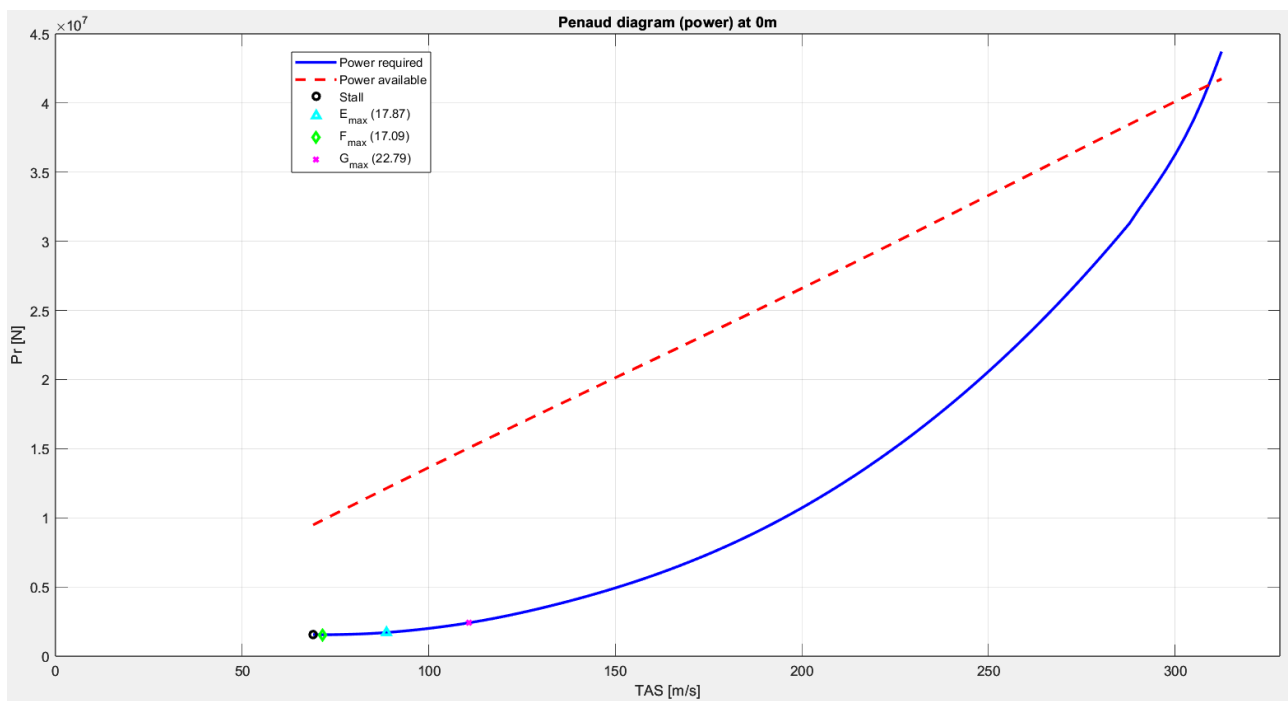
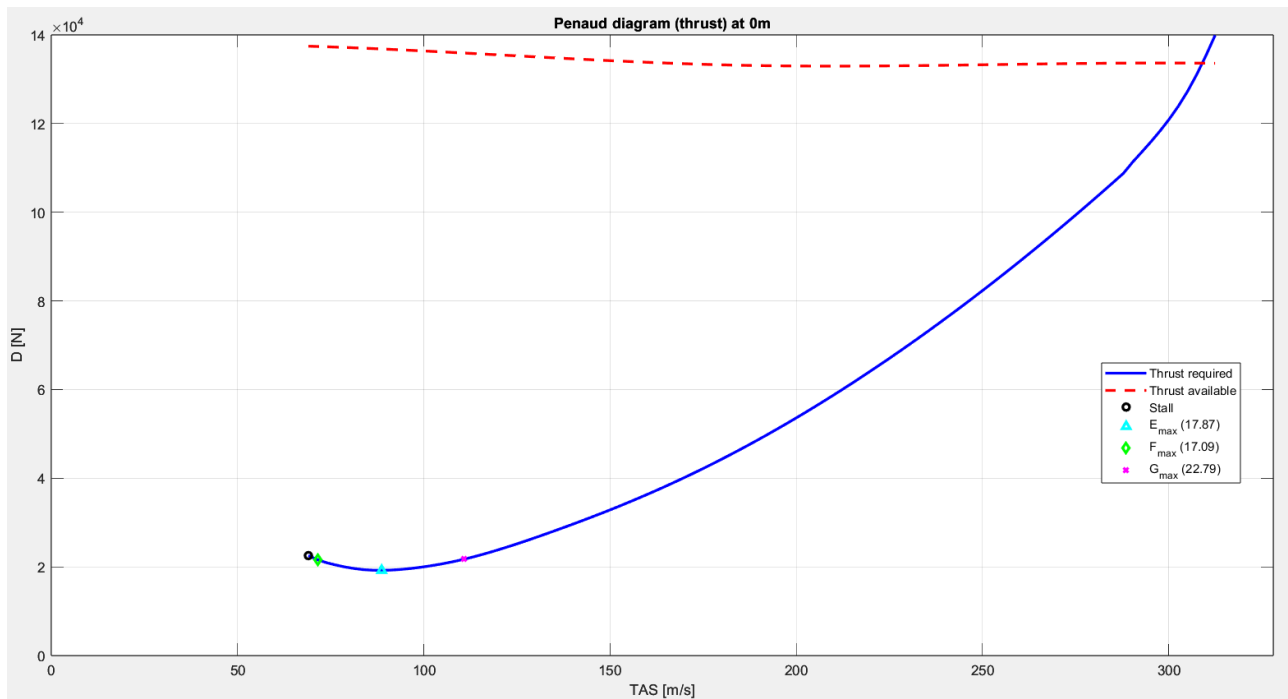
## 4. Level flight performances

Once the altitude is set (air parameters determined through the function *isatm*), it is possible to obtain the lift coefficient  $C_L = \frac{W/S}{1/2\rho V^2}$  from the vertical equilibrium for every selected airspeed

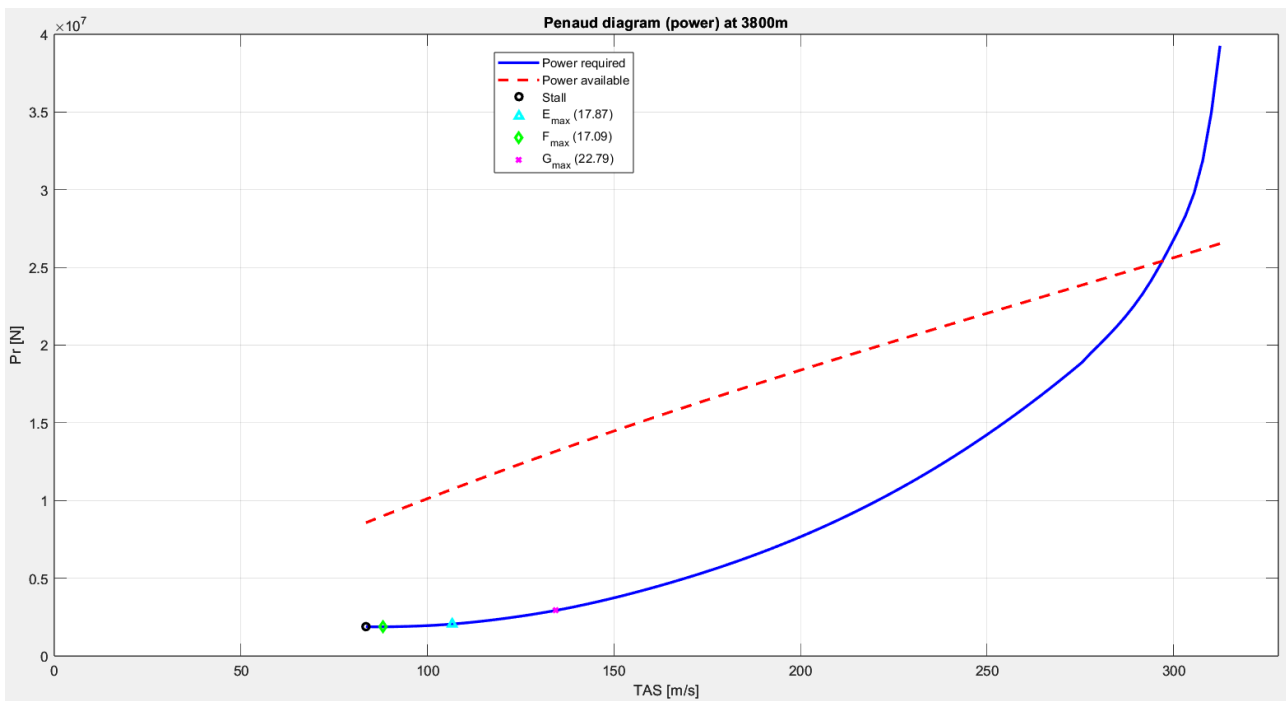
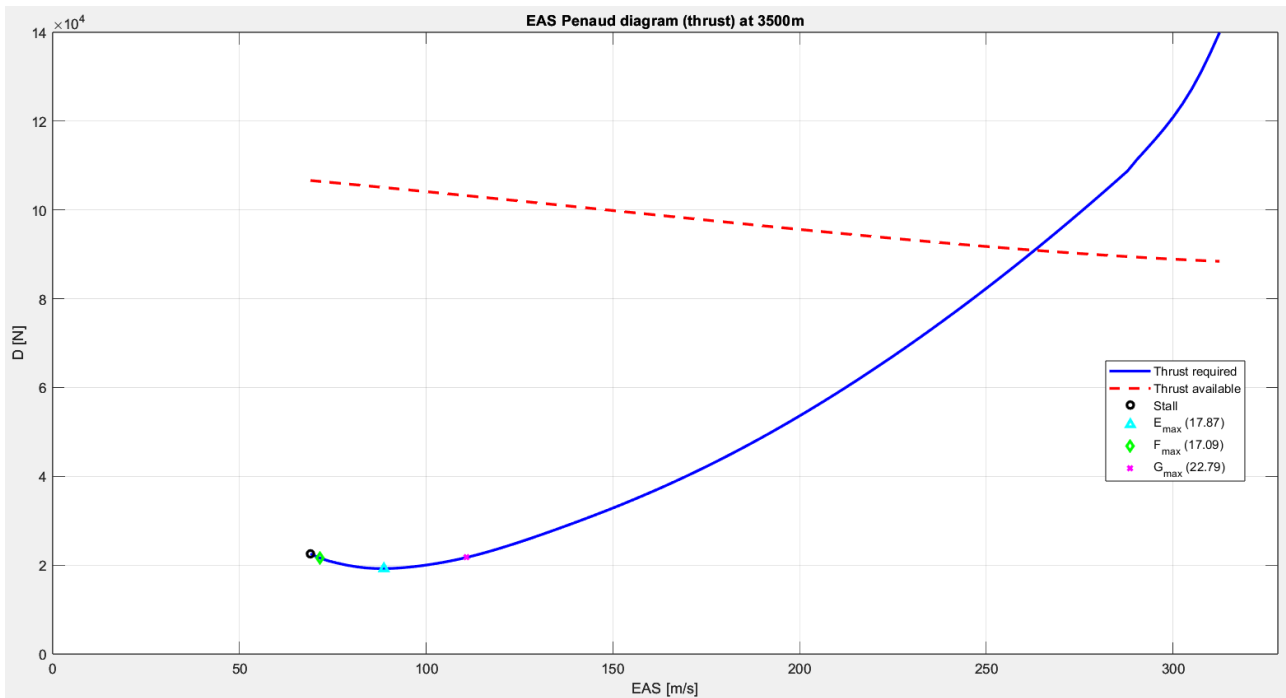
between  $V_{stall} = \sqrt{\frac{W/S}{1/2\rho C_{L,max}}}$  and the maximum speed. It is then possible to obtain the drag coefficient from the trimmed polar (adding the eventual drag-rise) and determine the drag and the required power:

$$D = 1/2\rho V^2 S C_D \quad P_r = 1/2\rho V^3 S C_D.$$

### 4.1



## 4.2



## 5. Climb performances

The climb performance analysis is made with the hypothesis of a steady, trimmed flight. To further simplify procedures, the hypothesis of a climb angle  $\gamma \ll 1$  makes the thrust required for horizontal flight an adequate approximation for the thrust required for climb. From the vertical equilibrium equation:

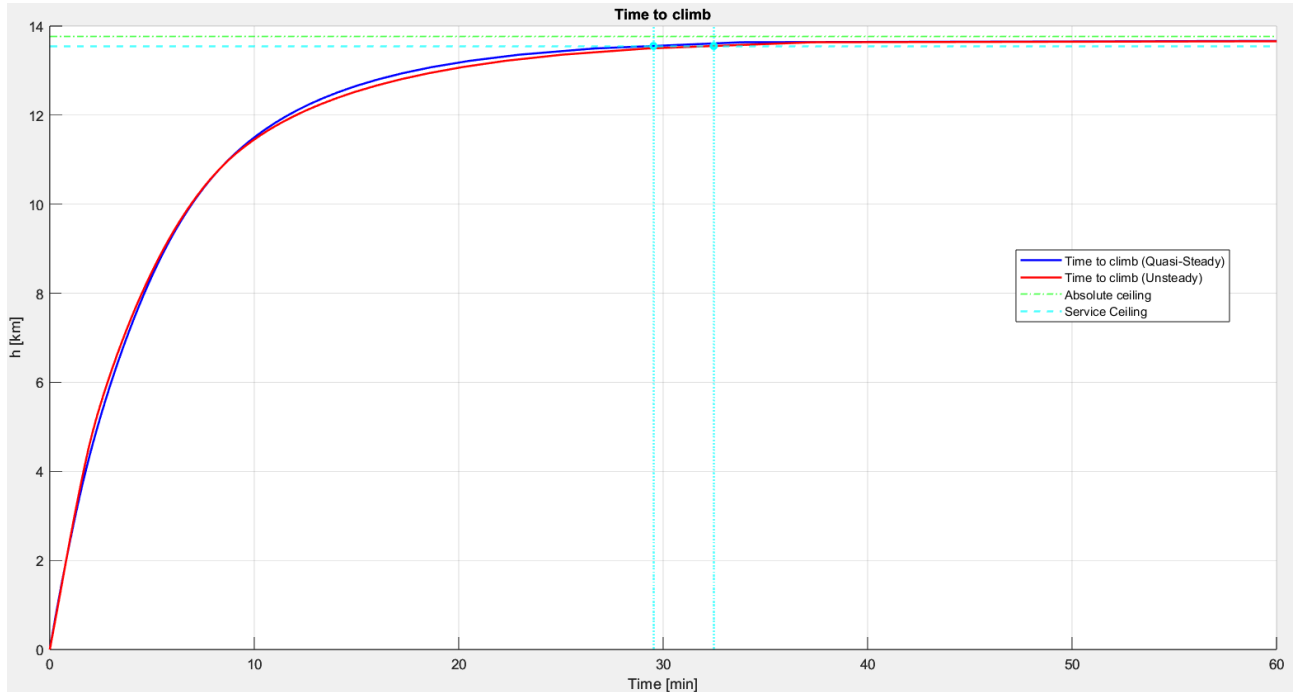
$$\begin{cases} T = D + W \sin \gamma \\ L = W \cos \gamma \end{cases} \rightarrow \begin{cases} \sin \gamma = (T - D)/W \\ L = W \end{cases}$$

By computing drag and required power at each altitude for all airspeeds it is possible to calculate

$$SET(V) = \frac{T(V) - D(V)}{W} \quad SEP(V) = \frac{P_a(V) - P_r(V)}{W}$$

As the climb requires a  $SET > 0$ , it is possible to determine the absolute ceiling by employing the bisection method: by evaluating the SET at the middle of the height interval to determine if it is positive, it is possible to know if the absolute ceiling is higher or lower than the selected height. The service ceiling is instead defined as the height at which the aircraft can no longer maintain a rate of climb higher than  $100 \text{ ft/min}$ .

### 5.1



The time to climb  $\tau_{\text{climb}} = \int_{t_1}^{t_2} dt = \int_{h_1}^{h_2} \frac{dh}{V_V(V, h)}$  necessitates of a numerical computation procedure that defines a grid of times and altitudes and replaces every derivative with its finite difference approximation.

The minimum time to climb can be computed either as:

$$\tau_{\text{quasi-steady}}^{\min} = \int_{h_1}^{h_2} \frac{dh}{\max_v SEP(V, h)} \quad \tau_{\text{unsteady}}^{\min} = \int_{h_1}^{h_2} \frac{dh}{\max_v \left( \frac{SEP}{1 + \frac{V dV}{g dh}} \right)}$$

The quasi-steady approach is based on the approximation:

$$V_v \approx SEP = \frac{P_a - P_r}{W}$$

Therefore, the time increase is computed as

$$\Delta t_k = \frac{h_k - h_{k-1}}{\max_V SEP(V, h_k)}$$

Instead, the unsteady approach takes the SEP's time dependence into account:

$$SEP = \frac{P_a - P_r}{W} = V_v + \frac{V}{g} \dot{V}$$

As

$$\dot{V} = \frac{dV}{dt} = \frac{dV}{dh} \frac{dh}{dt} = \frac{dV}{dh} \dot{h} = \frac{dV}{dh} V_v$$

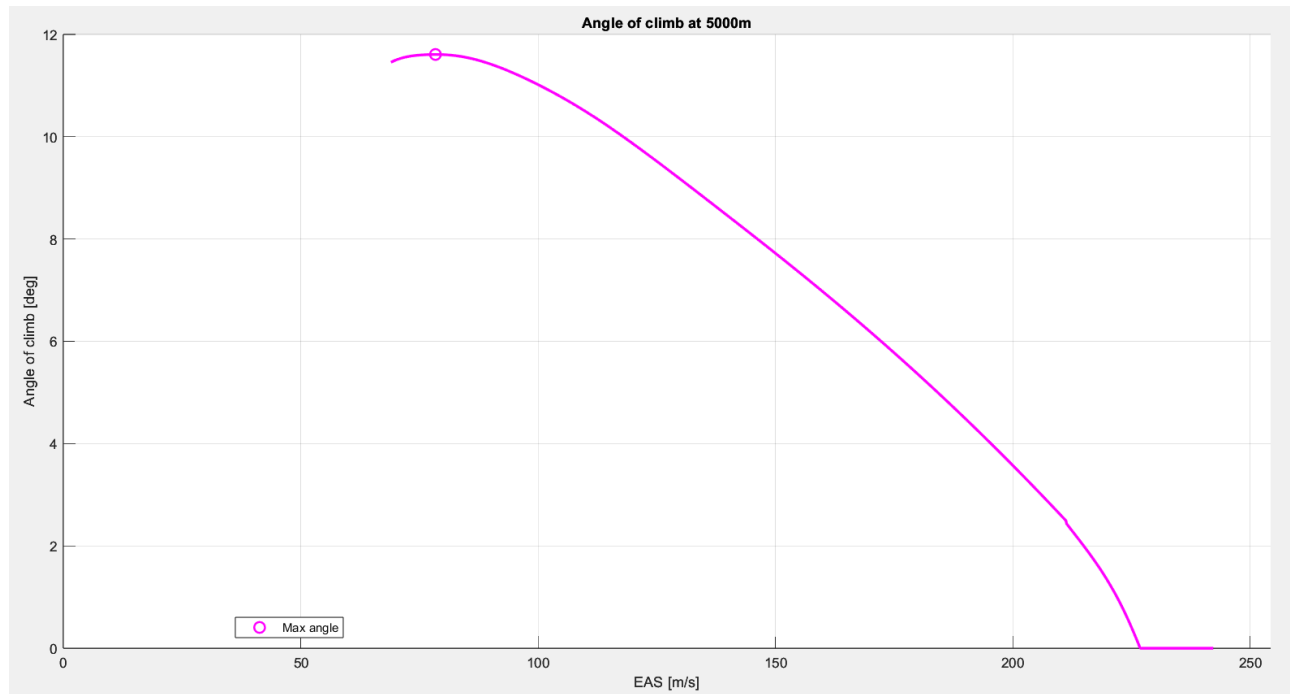
the vertical speed can be written as

$$V_v = \frac{SEP}{\left(1 + \frac{V}{g} \frac{dV}{dh}\right)}$$

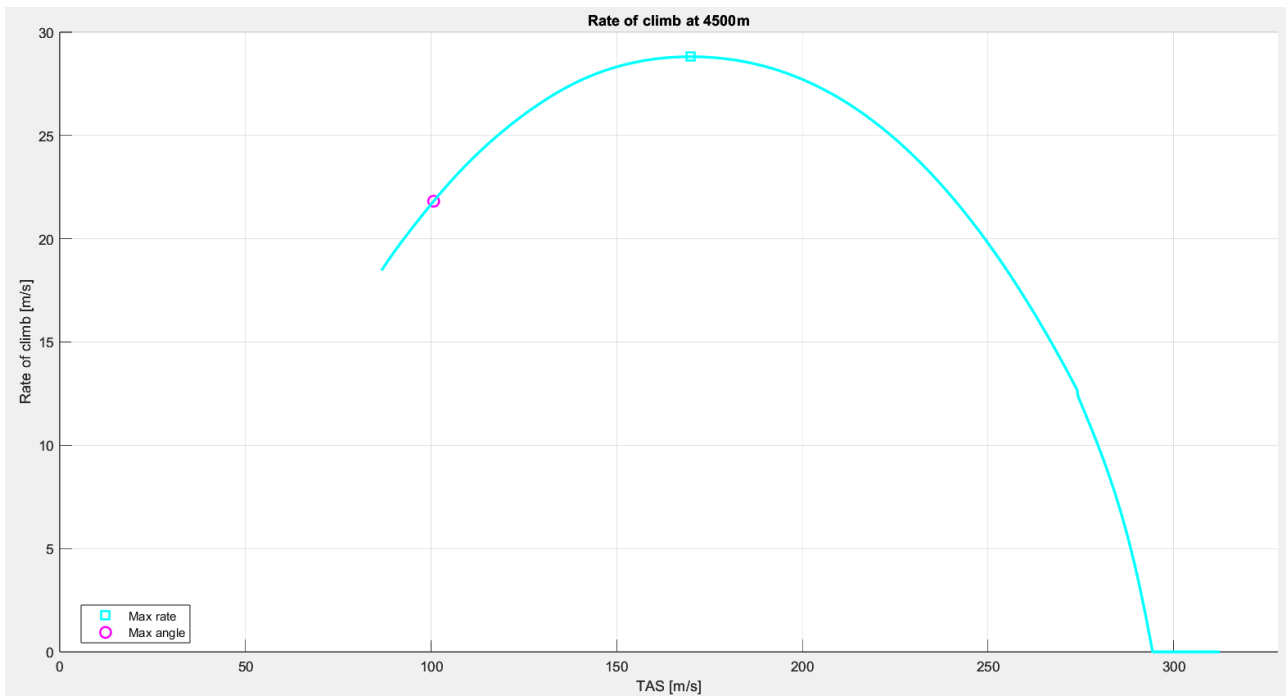
## 5.2

Parameter	Value	Unit
Theoretical ceiling	13776	m
Service ceiling	13554	m

## 5.3



As  $\gamma \ll 1$ ,  $\sin \gamma \approx \gamma$ . At a set altitude the angle of climb the be computed as  $\gamma = SET(V)$ .



As  $V_v = V \sin \gamma$ , at a set altitude the rate of climb can be computed as  $V_v = SEP(V)$ .

## 6. Flight envelope with climb performances

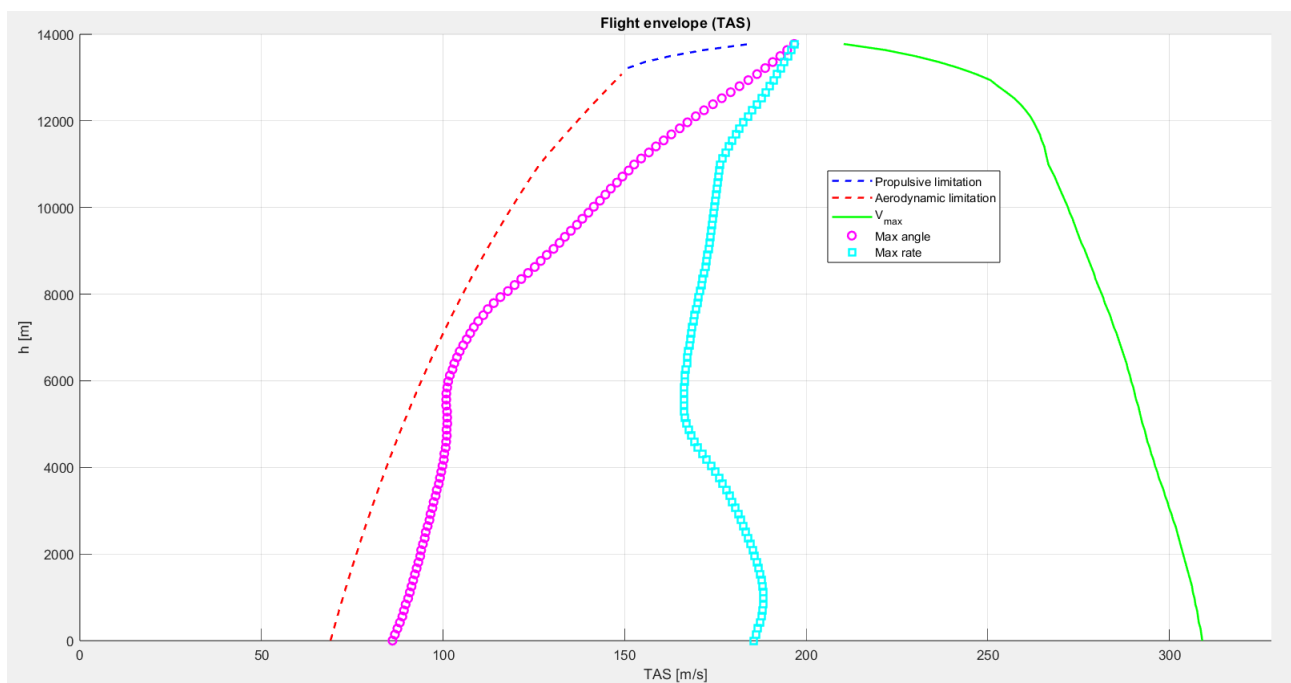
The flight envelope is determined by seeking, for every altitude, the airspeed values such that:

$$SET(V_{eq}) = \frac{T(V_{eq}) - D(V_{eq})}{W} = 0$$

In practice, a tolerance is set for the search to take the discretization into account.

As every altitude presents two equilibrium points (coinciding for the ceiling), at every height the speed domain is divided into two intervals by the maximum rate of climb speed. If no equilibrium point is found for the lower speed interval, the stall speed will be set as the equilibrium speed (aerodynamic limitation), if it is found the limitation is set as propulsive.

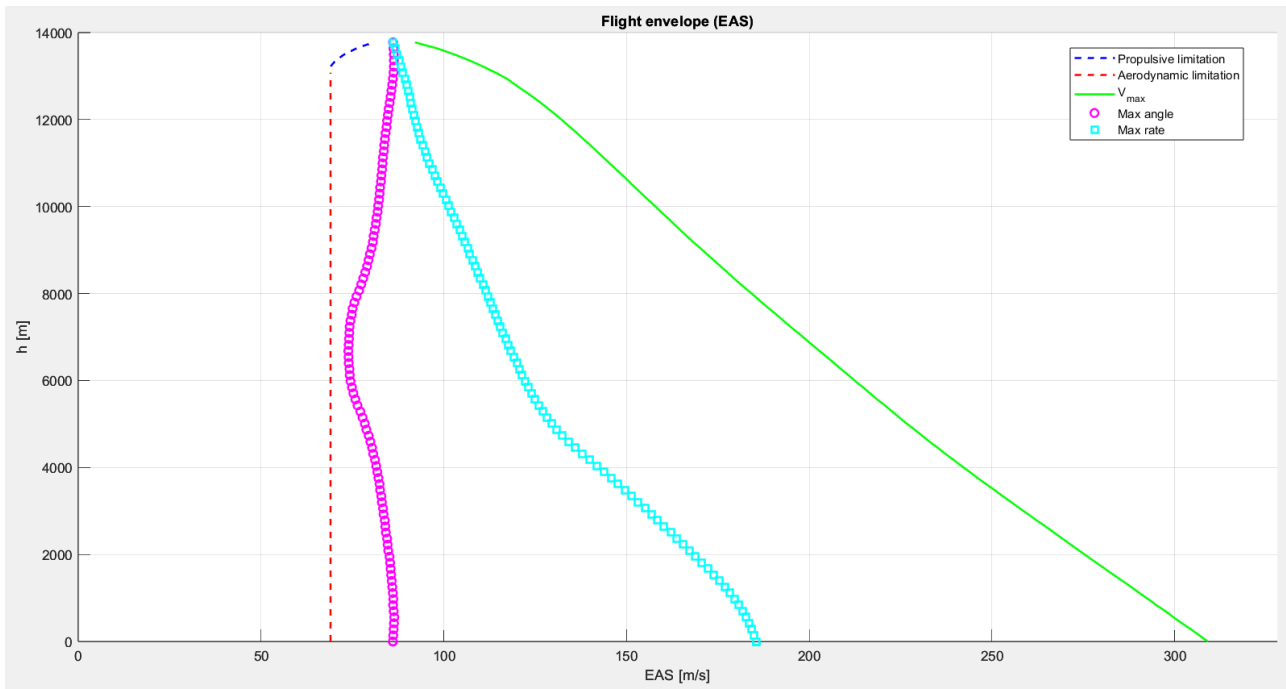
### 6.1



The flight envelope highlights, as the Penaud diagrams, a significative excess of thrust at lower altitudes that only becomes a limiting factor when nearing the absolute ceiling.

This is in line with the performance characteristics needed for an aircraft of this category, for which climb performance can greatly affect the operative flexibility.

## 6.2



The TAS to EAS conversion takes the decreasing air density into account as the aircraft ascends:

$$V_{EAS} = V_{TAS} \sqrt{\frac{\rho}{\rho_0}}$$

The EAS is defined as the airspeed at sea level under standard atmospheric conditions that would produce the same dynamic pressure as the current TAS at the selected altitude.

Maintaining a constant EAS results in the same dynamic pressure on the wings and control surfaces, regardless of altitude, as shown in the constant stall speed.

## 7. Turning performances

The equilibrium for a coordinate turn is described as:

$$\begin{cases} T = D \\ L \cos \phi = W \\ L \sin \phi = mV^2/R \\ M_G = 0 \end{cases}$$

Having defined the load factor as  $n = \frac{L}{W} \rightarrow n = 1/\cos\phi$ , the resulting system is comprised of:

- 8 scalar equations: 4 equilibriums, 1 load factor, 3 aerodynamics.
- 12 unknowns:  $\rho, V, \delta_T, C_D, C_L, C_{m_G}, W, \phi, R, n, \alpha, \delta_E$

Using the pitch moment equilibrium, it is possible to define  $\delta_E$  as a function of  $\alpha$ . The aerodynamic coefficients are therefore only dependent on  $\alpha$ . Additionally, the polar curve offers a relation between  $C_L$  and  $C_D$ , bringing the balance to 5 equations and 9 unknowns.

By neglecting the thrust-drag equilibrium we additionally remove 2 equations and 2 parameters.

Assigning  $\rho, W, V$  will result in only one parameter to be chosen among  $n, \phi, R$ .

Having chosen the load factor:

$$\begin{cases} \phi = \cos^{-1}\left(\frac{1}{n}\right) \\ C_L = \frac{2nW}{\rho SV^2} \\ R = \frac{V^2}{g\sqrt{n^2 - 1}} \end{cases}$$

The turn performances of an aircraft are subject to three limiting effects:

- Aerodynamic limit → Stall
- Propulsive limit → Available thrust
- Structural/Regulation limit → Maximum load factor

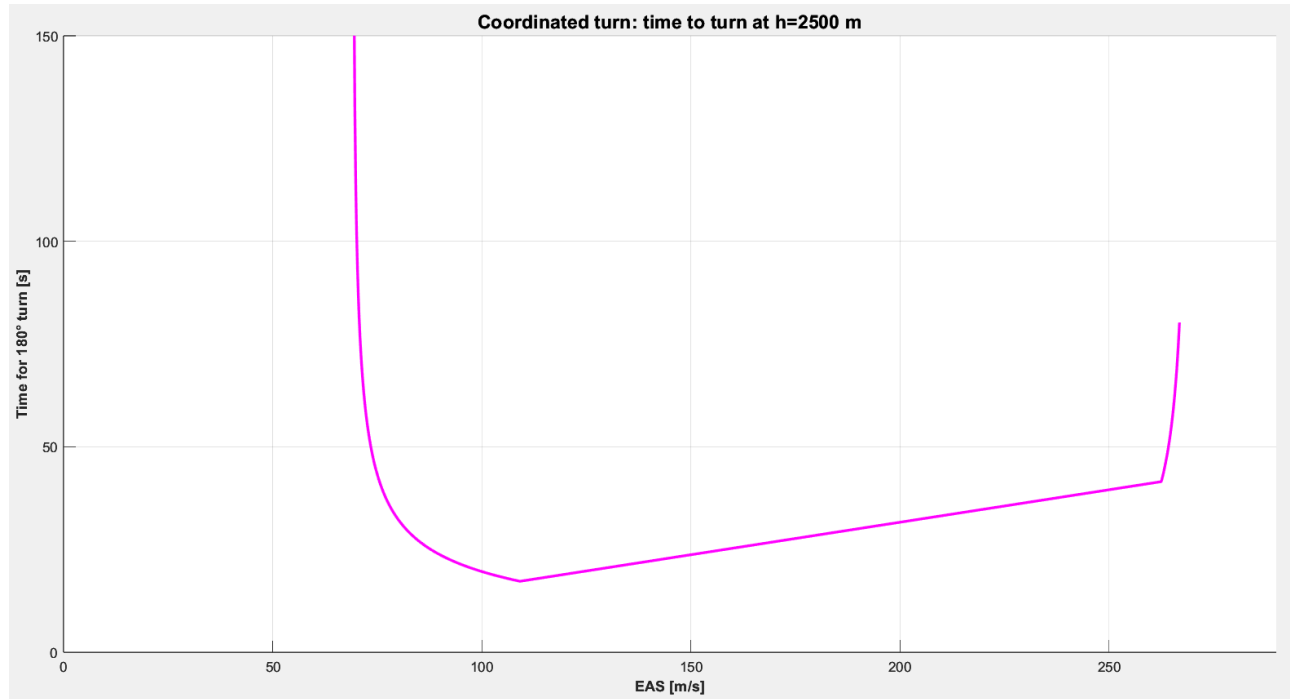
Where the maximum load factor for civil aircraft is typically equal to 2.5.

The turn performances can be evaluated through performance indicators:

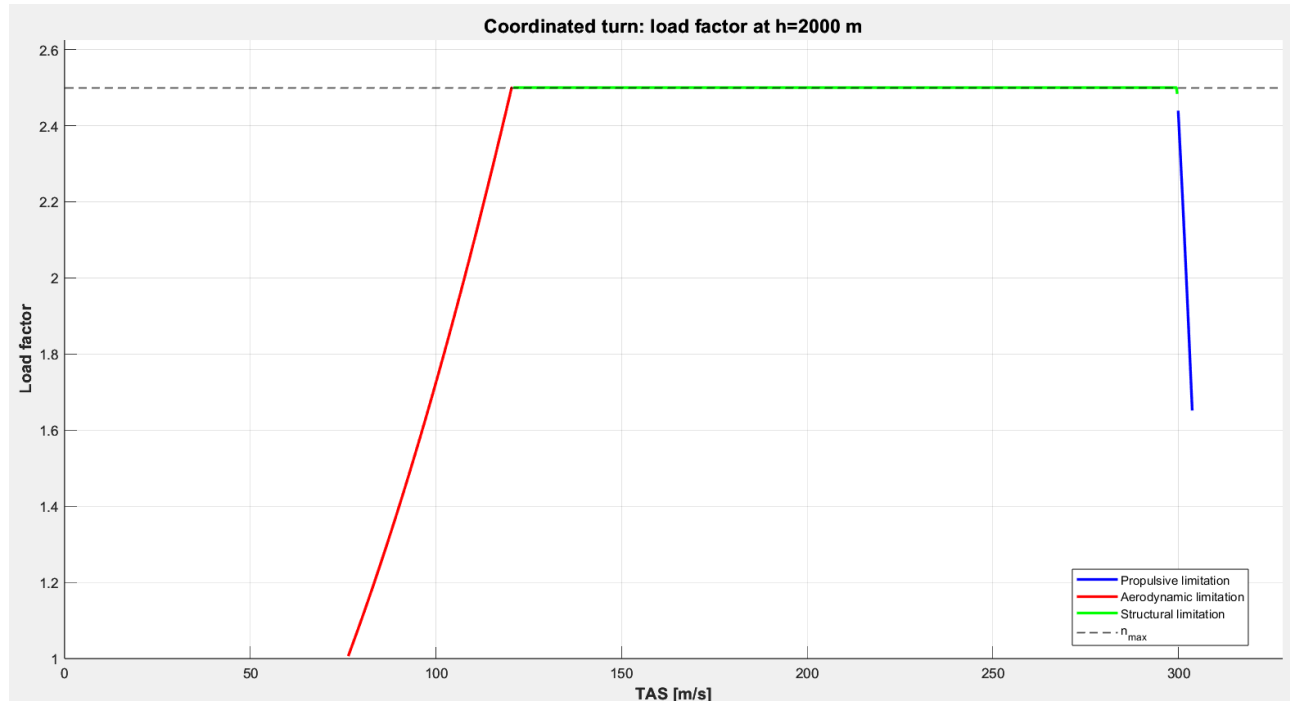
- Bank angle:  $\phi = \cos^{-1}(1/n)$
- Turn radius:  $R = \frac{V^2}{g\sqrt{n^2 - 1}}$
- Turn rate:  $\Omega = V/R$
- Turn time:  $\tau_\pi = \pi/\Omega$

At a desired speed, the optimal performance is always associated with the maximum achievable load factor.

## 7.1



At a set altitude, the time to turn is calculated by computing the turn radius:  $R = \frac{V^2}{g\sqrt{n^2-1}}$ , from which the turn rate is defined as  $\Omega = V/R$ . Finally, the time for a  $180^\circ$  turn is:  $\tau_\pi = \pi/\Omega$ . The minimum point of the curve is the best turning performance point, while at the edges of the speed interval the time to turn goes to infinite.



Having set an altitude and a flight speed in the level flight speed interval  $V_{min} \leq V \leq V_{max}$ , the current active limitation can be determined with the following procedure:

1. A propulsive limitation is assumed at first.

By computing the drag coefficient as  $C_D = \frac{T}{\frac{1}{2}\rho V^2 S}$  and excluding the contribution of the drag-rise it is possible to determine the lift coefficient by interpolating the polar.

2. If  $C_L > C_{L_{max}}$  then  $C_L = C_{L_{max}}$  is imposed and the active limitation is set as aerodynamic.

3. To verify the structural limitation, the load factor is computed as  $n = \frac{\frac{1}{2}\rho V^2 S C_L}{W}$ .

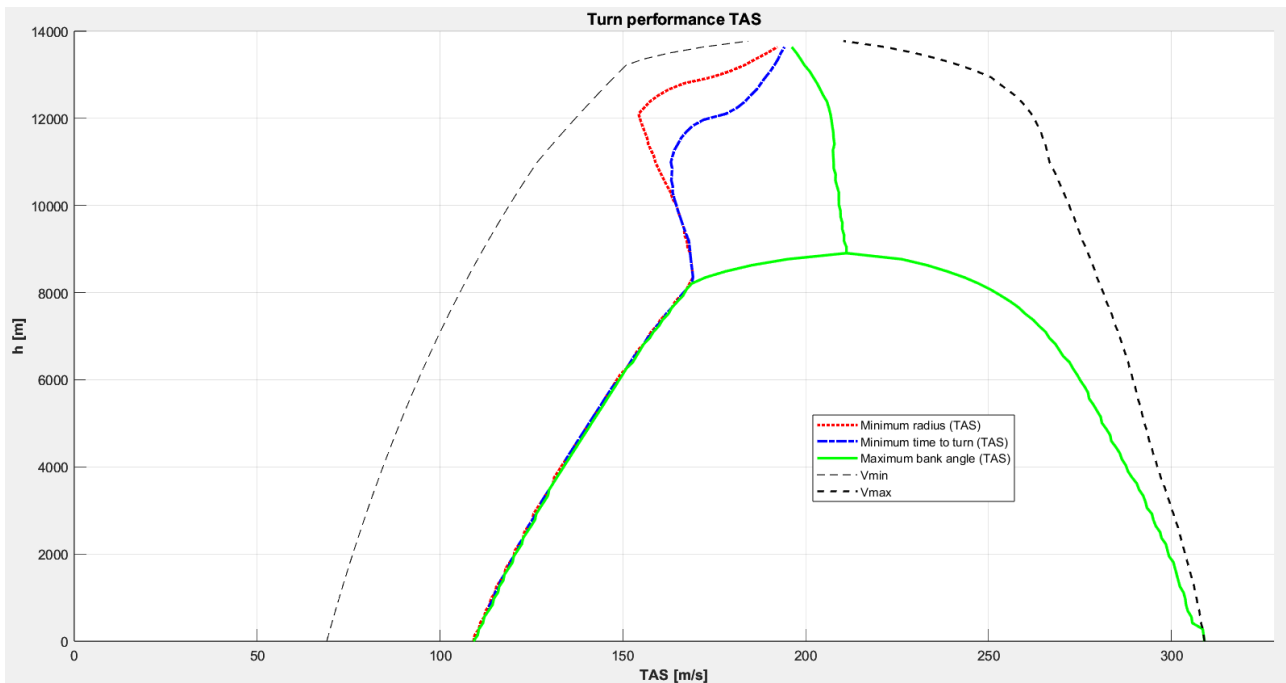
If  $n > n_{max}$  then  $n_{TURN} = n_{max}$  is imposed and the active limitation is set as structural, otherwise  $n_{TURN} = n_{max}$

It is then possible to compute the turn radius and time to turn using  $n_{TURN}$  and  $V$ .

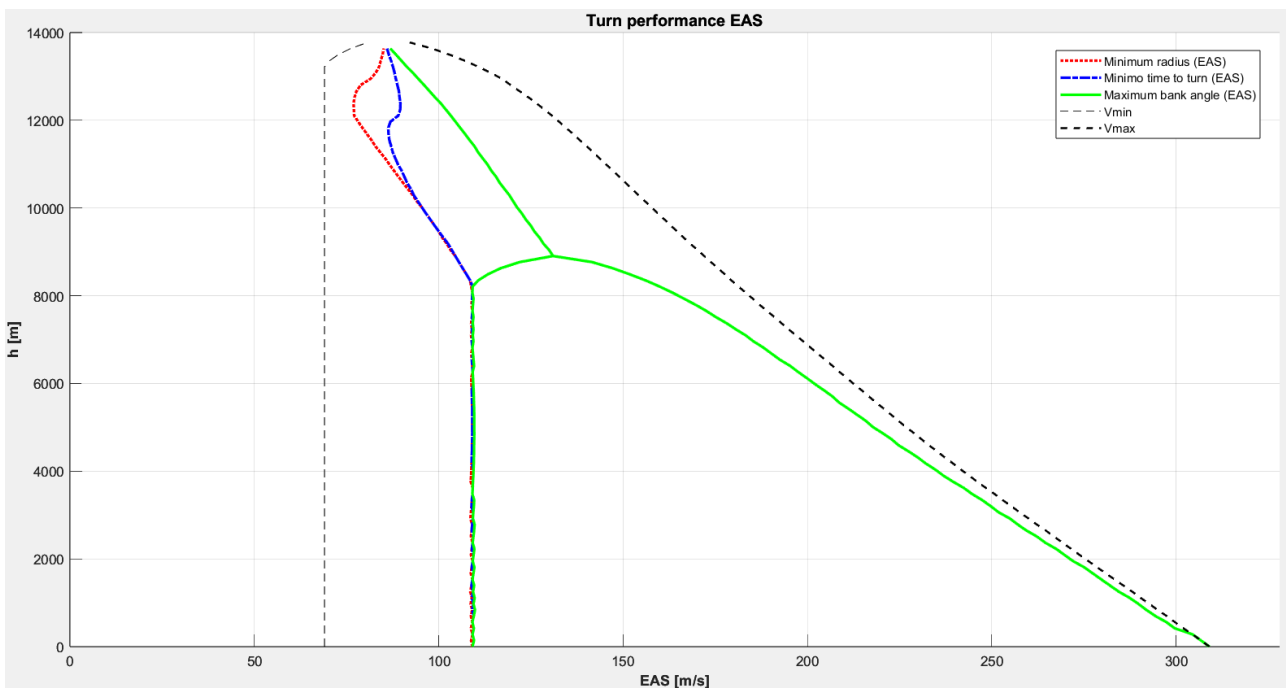
## 8. Flight envelope in coordinated turn

The turning performance indicators can be evaluated at a range of altitudes, offering a broader view of the plane's turning performance.

### 8.1

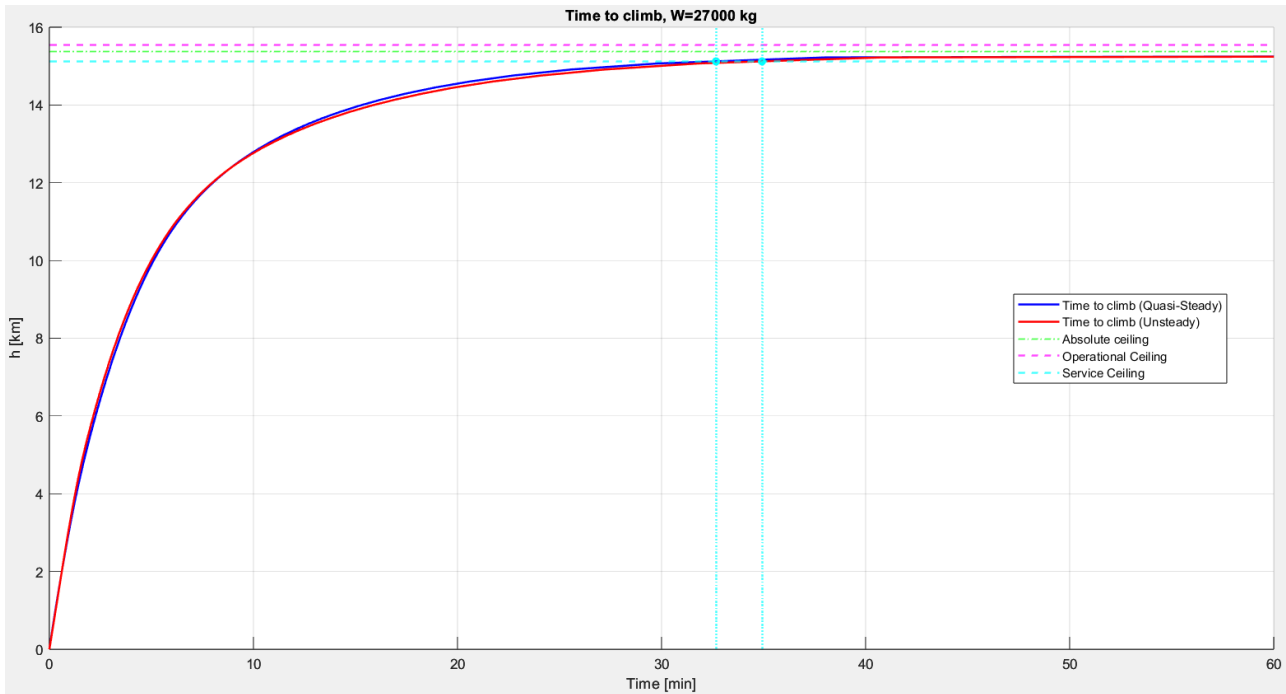


### 8.2



## 9. Additional results

### 9.1

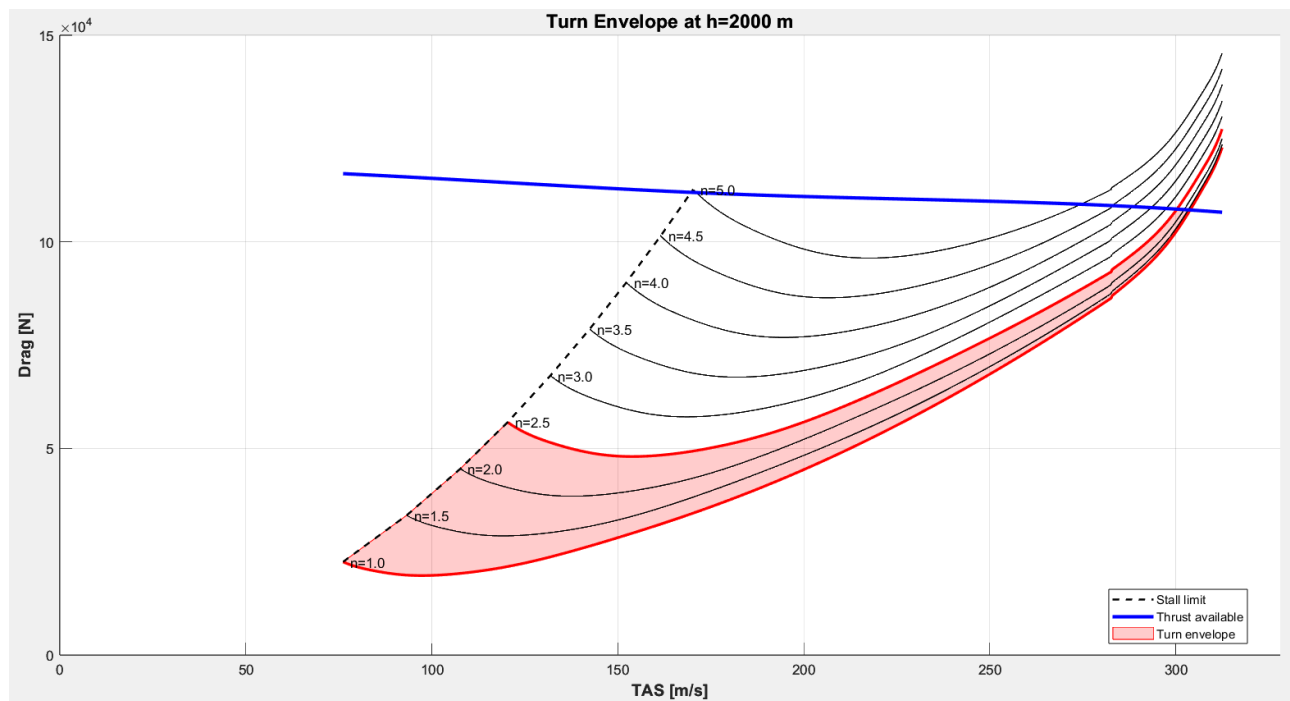


The considered weight of 35,000 kg is typical for the earlier stages of the mission (from take-off to the initial stages of the cruise) and was chosen to offer more representative results of all the conditions and manoeuvres analysed.

As fuel is consumed during the flight, the weight of the aircraft is gradually reduced. As weight directly impacts the flight performances, the absolute ceiling is also affected. In a realistic scenario, the cruise altitude is adjusted during the flight to take the weight reduction into account: a lower weight allows a higher ceiling.

The manufacturer cites an operational ceiling of 15,545 m which is in line with the figures found by setting a weight of 27,000 kg, reasonable for the later stages of a cruise.

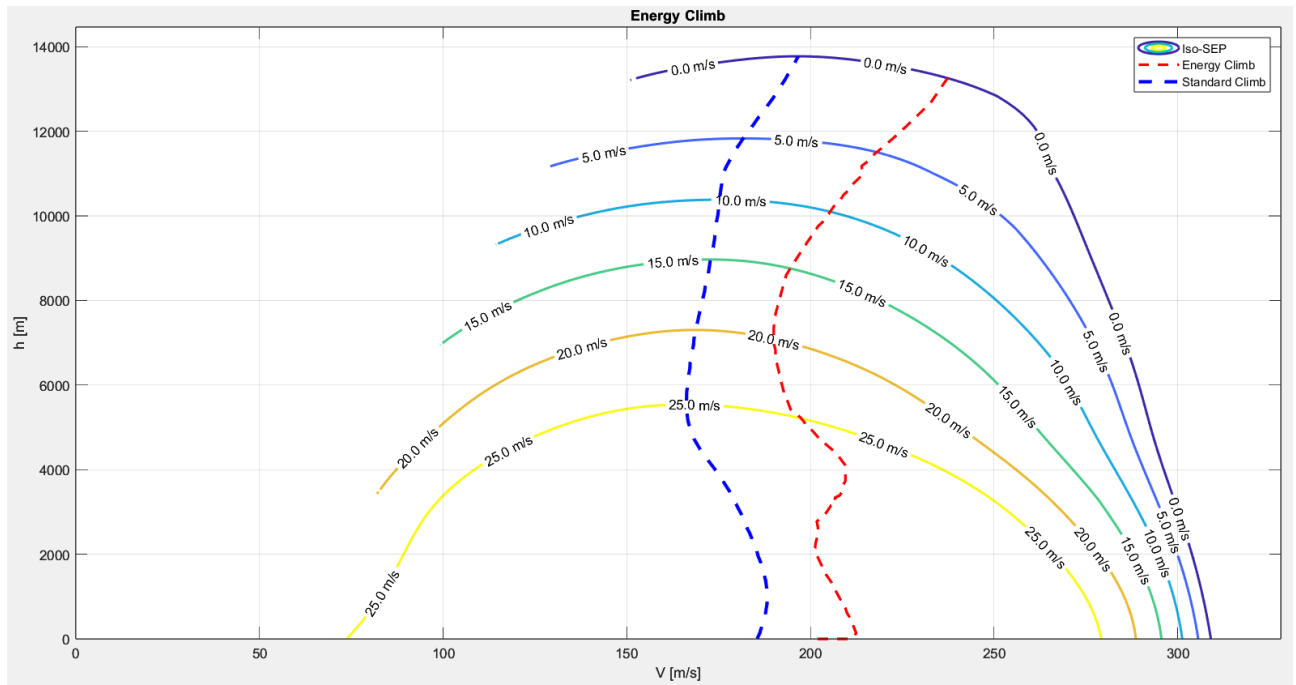
## 9.2



The turn envelope shows the conditions at which a coordinated turn is possible.

By repeating the computation for the drag at different load factors it is possible to determine the limiting conditions to the turn. As seen previously, also in this case the thrust is a limiting factor only at the highest speeds while the main limiting factor is the maximum load factor.

## 9.3



Having defined the minimum time to climb with a steady climb as:

$$\min(\tau_C) = \int_{h_1}^{h_2} \frac{dh}{\max(\text{SEP})}$$

It is possible to perform a change of variable through the energy height  $H = h + \frac{V^2}{2g}$ :

$$\min(\tau_C) = \int_{H_1}^{H_2} \frac{dH}{\max(\text{SEP})}$$

To minimize the time to climb it is necessary to maximize the SEP at each energy height.

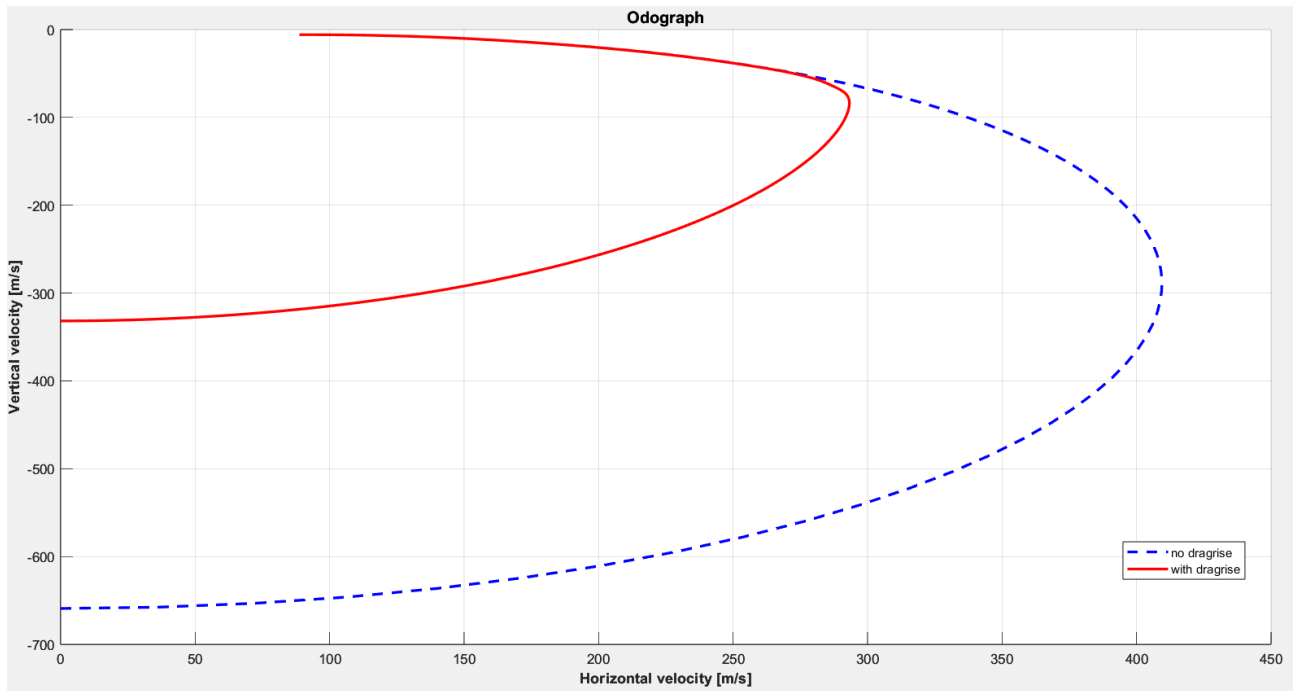
To determine the energy climb path it is necessary to define the iso-SEP lines and determine the points where they are tangent to the iso-H lines.

- A grid of heights and speeds is defined. The SEP is calculated for every point of the grid.
- The iso-SEP curves are defined via the MATLAB function  $C = \text{contourc}(X, Y, Z, [v, v])$  which computes the contours at the selected SEP level. The matrix C stores the information relative to the selected iso-SEP curve: the values in the first column indicate the level of the first contour line and the number of vertices, while the following columns store the coordinates of the vertices. The data of the following SEP levels is stored in the same manner, with a header followed by the coordinates one after the other.

To extract and order the points of the contour the function  $[x, y] = \text{extractContour}(C)$  is defined: the header gives information on the number of points to acquire for every SEP level, while the coordinates itself are sorted to create a coherent coordinates vector.

- To determine the tangent points, the code computes the slope of the iso-SEP curves point for point and searches for the closest to the slope of the energy height curve  $-V/g$ .

## 9.4



The calculations for gliding flight are done utilizing the same equations used for the climb, but with null thrust and without the  $\gamma \ll 1$  hypothesis, resulting in:

$$\begin{cases} L = W\cos\gamma \\ D = -W\sin\gamma \end{cases} \rightarrow SET < 0, SEP < 0, \gamma < 0$$

Having defined the descend angle  $\gamma_D = -\gamma$  and the descend speed  $V_D = -V_V$ :

$$\tan\gamma_D = \frac{1}{E} \quad V_D = \frac{P_r}{W}$$

The odograph displays the steady flight conditions of a glider. Having assumed fixed altitude and weight, for an assigned lift coefficient it is possible to determine the drag coefficient from the polar and compute  $\gamma_D$ . From the vertical equilibrium:

$$V = \sqrt{\frac{\cos(\gamma_D)W}{\frac{1}{2}\rho S C_L}}$$

From which it is possible to determine the vertical and horizontal velocity:

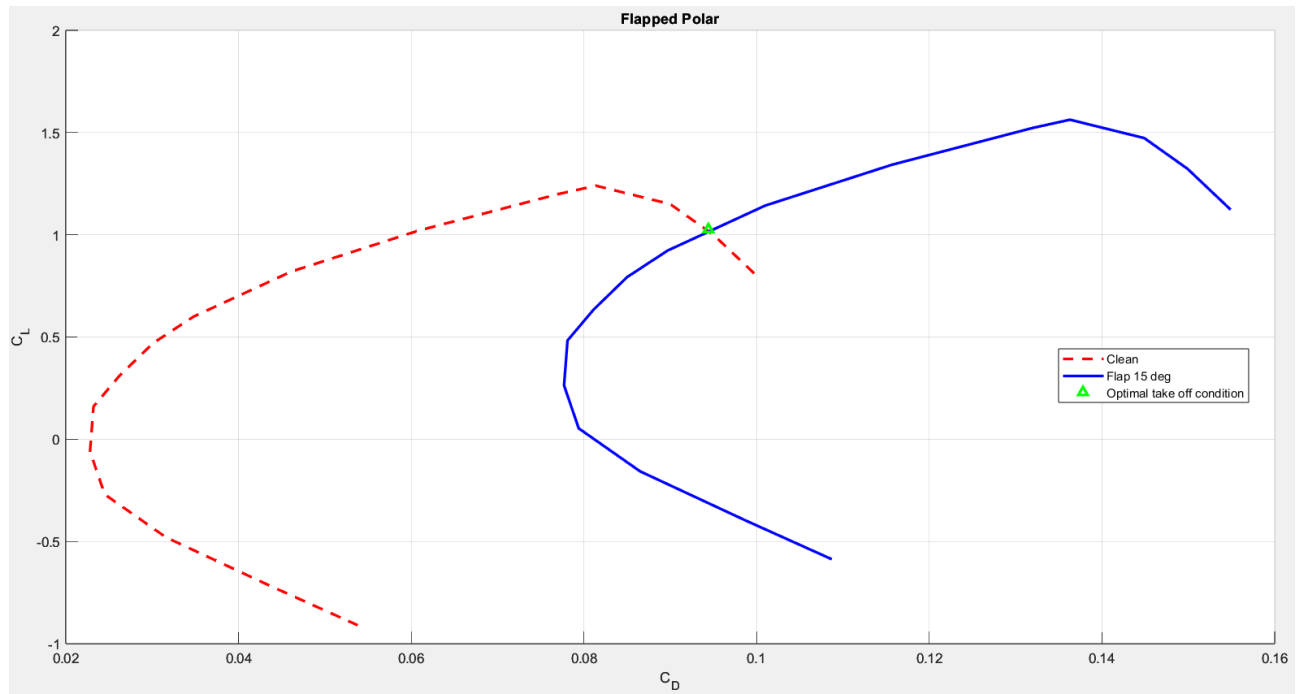
$$V_H = V\cos(\gamma_D) \quad V_D = V\sin(\gamma_D)$$

To take the drag-rise into account, the procedure is analogue, but it is necessary to solve a nonlinear problem:

$$\begin{cases} f_1 = \frac{1}{2}\rho V^2 S C_L - W\cos(\gamma_D) = 0 \\ f_2 = \frac{1}{2}\rho V^2 S(C_D(C_L) + \Delta C_D(V/c)) - W\sin(\gamma_D) = 0 \end{cases}$$

By using the *fsoolve* function it is possible to determine  $\gamma_D$  and  $V$  for the assigned lift coefficient.

## 9.5



To determine take-off performances, it is necessary to derive the flapped polars. The employed method is taken from “Roskam, *Airplane Design*, Roskam Aviation, 1985”.

While some of parameters used for this method are tabulated coefficients, others are assumptions derived from estimates based on available technical drawings and images.

Flapped polar		
Parameter	Value	Unit
$K_{\text{interference}}$	0.25	-
$K_{\text{induced}}$	0.08	-
$\delta_{\text{flaps}}$	15	deg
$\Lambda_{c/4}$	35	deg
$S_{\text{flapped}}/S$	0.85	-
$c_{\text{flap}}/c$	0.2	-
$\Delta C_{D_{2D}}$	0.005	-
$C_{L_{\delta_f}}$	3.75	-
$K'$	0.95	-
$\Delta C_{D_{\text{gear}}}$	0.05	-

- Estimation of lift increment:

$$\Delta C_{L_{max}} = \Delta C_{L_{airfoil}} \frac{S_{flapped}}{S} K_\Lambda$$

Where

$$K_\Lambda = (1 - 0.08 \cos^2 \Lambda_{c/4}) \cos^{3/4} \Lambda_{c/4}$$

Is the correction for the wing's sweep angle, while

$$\Delta C_{L_{airfoil}} = C_{L_{\delta_f}} \delta_{flaps} K'$$

Is the airfoil's lift increase, with  $C_{L_{\delta_f}}$  and  $K'$  tabulated coefficients for Fowler flaps.

- Estimation of drag increment:

$$\Delta C_{D_f} = \Delta C_{D_{f_{airfoil}}} + \Delta C_{D_{f_{induced}}} + \Delta C_{D_{f_{interference}}} + \Delta C_{D_{gear}}$$

Where

$$\Delta C_{D_{f_{airfoil}}} = \Delta C_{D_{2D}} \cos \Lambda_{c/4} \frac{S_{flapped}}{S}$$

Is the increment of the isolated airfoil

$$\Delta C_{D_{f_{induced}}} = K_{induced}^2 \Delta C_{L_{max}}^2 \cos \Lambda_{c/4}$$

Is the increment induced by lift

$$\Delta C_{D_{interference}} = K_{interference} \Delta C_{D_{f_{airfoil}}}$$

Is the interference drag, with  $\Delta C_{D_{2D}}$ ,  $K_{induced}$  and  $K_{interference}$  tabulated coefficients for Fowler flaps and  $\Delta C_{D_{gear}}$  tabulated coefficient for the drag produced by the landing gear.

For the ground run, the equilibrium references a runway-specific frame:

$$\begin{cases} m\dot{V} = T - D - R_T - W \sin \psi_{RW} \\ 0 = L + R_N - W \cos \psi_{RW} \end{cases}$$

Where  $R_N$  and  $R_T$  are ground reaction forces linked through the friction coefficient as  $R_T = \mu R_N$ . By manipulating the equations:

$$\dot{V} = g \left( \frac{T}{W} - \frac{D - \mu L}{W} - (\mu + \psi) \right) = \frac{dV}{dt} \rightarrow dt = \frac{dV}{\dot{V}}$$

The ground run can be then computed as:

$$S_G = \int_{t_{IN}}^{t_{LO}} V dt = \int_{V_{IN}}^{V_{LO}} \frac{V}{\dot{V}} dV = \frac{1}{g} \int_{V_{IN}}^{V_{LO}} \frac{V dV}{\frac{T}{W} - \frac{D - \mu L}{W} - (\mu + \psi)}$$

By performing a change of variable:

$$\xi = \frac{V}{V_{LO}} \rightarrow dV = V_{LO} d\xi$$

As  $C_{L_{LO}} = \frac{1}{1.1} C_{L_{stall}}$  and  $V_{LO} = \sqrt{1.1} V_{stall}$ , the expression for the ground run can be written as:

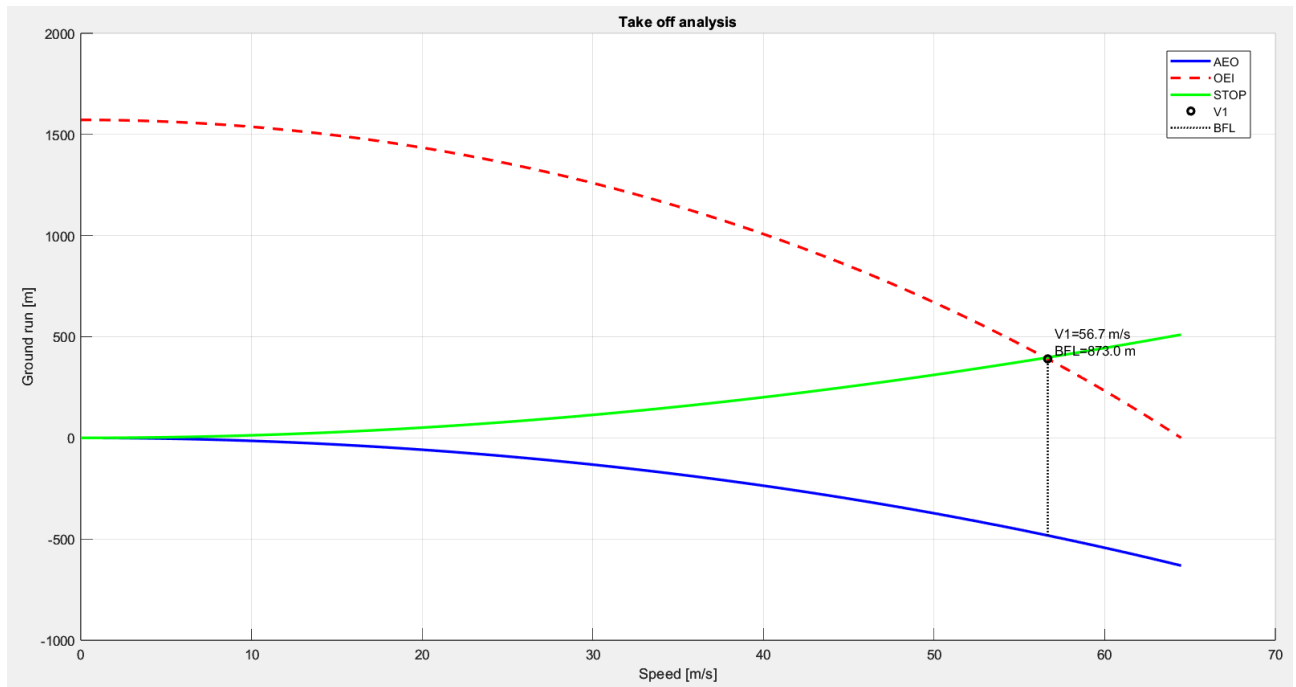
$$S_G = \frac{W/S}{g} \int_{\xi_{IN}}^1 \frac{\xi d\xi}{\frac{1}{2} \rho \frac{1}{1.1} C_{L_{stall}} \left( \frac{T}{W} - (\mu + \psi) \right) - \frac{1}{2} \rho \xi^2 (C_D - \mu C_L)}$$

The value  $\mu = 0.05$  is reasonable for a dry asphalt/concrete runway, while for simplicity the runway's inclination  $\psi$  is assumed null.

To determine the optimal lift and drag coefficients for the ground run it is necessary to find the minimum point of  $C_D - \mu C_L$ , which can be achieved through the flapped polar.

The resulting ground run is of  $S_G = 631.3m$ .

## 9.6



By using the ground run model, it is possible to evaluate the decision speed  $V_1$  (defined as the speed at which, in the event of an engine failure, the distance required to continue the take-off is equal to the distance required to abort it) and balance field length BFL (defined as the sum of the distance required to accelerate till  $V_1$  with all engines operative and the distance required to stop the plane from  $V_1$  with one engine inoperative).

For the computation, some assumptions are made: the runway angle is considered null, for simplicity the drag of the windmilling engine, the thrust reversal and the airbrakes are not considered.

- AEO (all engines operative):

At full throttle. The polar used is the one previously calculated for take-off conditions.

$$S_{AEO}(\bar{V}) = - \int_{V_{IN}}^{\bar{V}} \frac{V}{\dot{V}} dV$$

- OEI (one engine inoperative):

Thrust is halved. For a more rigorous approach, the polar should include the contribution of the windmilling engine.

$$S_{OEI}(\bar{V}) = \int_{\bar{V}}^{V_{LO}} \frac{V}{\dot{V}} dV$$

- STOP (aborted take-off):

Thrust is null. For a more rigorous approach, the usage of thrust reversers and the contribution of the windmilling engine and the airbrakes is necessary. The attrition coefficient is increased to  $\mu_{brake} = 0.4$  as the brakes are applied.

$$S_{STOP}(\bar{V}) = - \int_{\bar{V}}^0 \frac{V}{\dot{V}} dV$$